Targeted disruption of PDE3B, but not PDE3A, protects murine heart from ischemia/reperfusion injury

Youn Wook Chung[a,b,1,2], Claudia Lagranha[c,1], Yong Chen[d], Junhui Sun[c], Guang Tong[c,e], Steven C. Hockman[a], Faiyaz Ahmad[a], Shervin G. Esfahani[f], Dahae H. Bae[f], Nazari Polidovitch[g], Jian Wu[g], Dong Keun Rhee[a], Beom Seob Lee[b,h], Marjan Gucek[d], Mathew P. Daniels[f], Christine A. Brantner[f], Peter H. Backx[g,i], Elizabeth Murphy[c], and Vincent C. Manganiello[a,2]

[a]Cardiovascular and Pulmonary Branch, [c]Systems Biology Center, [d]Proteomics Core Facility, and [f]Electron Microscopy Core Facility, National Heart, Lung, and Blood Institute, National Institutes of Health, Bethesda, MD 20892; [b]Yonsei Cardiovascular Research Institute, Yonsei University College of Medicine, Seoul 120-752, Korea; [e]Department of Cardiovascular Surgery, Guangzhou General Hospital of Guangzhou Military Command, Guangzhou, Guangdong 510010, China; [g]Departments of Physiology and Medicine, University of Toronto, Toronto, ON M5S 3A8, Canada; [h]Graduate Program in Science for Aging, Yonsei University, Seoul 120-752, Korea; and [i]Division of Cardiology, University Health Network, Toronto, ON M5S 3E2, Canada

Edited by Joseph A. Beavo, University of Washington School of Medicine, Seattle, WA, and approved March 13, 2015 (received for review August 29, 2014)

Although inhibition of cyclic nucleotide phosphodiesterase type 3 (PDE3) has been reported to protect rodent heart against ischemia/reperfusion (I/R) injury, neither the specific PDE3 isoform involved nor the underlying mechanisms have been identified. Targeted disruption of PDE3 subfamily B (PDE3B), but not of PDE3 subfamily A (PDE3A), protected mouse heart from I/R injury in vivo and in vitro, with reduced infarct size and improved cardiac function. The cardioprotective effect in PDE3B$^{-/-}$ heart was reversed by blocking cAMP-dependent PKA and by paxilline, an inhibitor of mitochondrial calcium-activated K channels, the opening of which is potentiated by cAMP/PKA signaling. Compared with WT mitochondria, PDE3B$^{-/-}$ mitochondria were enriched in antiapoptotic Bcl-2, produced less reactive oxygen species, and more frequently contacted transverse tubules where PDE3B was localized with caveolin-3. Moreover, a PDE3B$^{-/-}$ mitochondrial fraction containing connexin-43 and caveolin-3 was more resistant to Ca^{2+}-induced opening of the mitochondrial permeability transition pore. Proteomics analyses indicated that PDE3B$^{-/-}$ heart mitochondria fractions were enriched in buoyant ischemia-induced caveolin-3–enriched fractions (ICEFs) containing cardioprotective proteins. Accumulation of proteins into ICEFs was PKA dependent and was achieved by ischemic preconditioning or treatment of WT heart with the PDE3 inhibitor cilostamide. Taken together, these findings indicate that PDE3B deletion confers cardioprotective effects because of cAMP/PKA-induced preconditioning, which is associated with the accumulation of proteins with cardioprotective function in ICEFs. To our knowledge, our study is the first to define a role for PDE3B in cardioprotection against I/R injury and suggests PDE3B as a target for cardiovascular therapies.

PDE3B$^{-/-}$ mice | protein kinase A | ischemia/reperfusion injury | signalosome | membrane repair

The two cyclic nucleotide phosphodiesterase type 3 (PDE3) subfamilies PDE3A and PDE3B are products of separate but homologous genes. PDE3 isoforms hydrolyze both cAMP and cGMP with high affinity (K_m <1 μM) in a mutually competitive manner and are important regulators of cyclic nucleotide signaling pathways and responses in cardiomyocytes and vascular smooth muscle (1). PDE3A and PDE3B exhibit different patterns of expression. PDE3A is more abundant in platelets, airway and vascular smooth muscle, and cardiovascular tissues, whereas PDE3B is relatively more highly expressed in tissues that are important in regulating energy metabolism, including liver, pancreatic β cells, brown adipose tissue (BAT), and white adipose tissue (WAT) (2). Little is known about their differential localization and functions when PDE3A and PDE3B are present in the same cell. To gain further insight into specific PDE3A and PDE3B functions in physiological contexts, we have generated and studied PDE3A$^{-/-}$ and PDE3B$^{-/-}$ mice (3, 4).

PDE3 inhibitors, e.g., milrinone, are thought to enhance myocardial inotropic responses via cAMP/PKA regulation of Ca^{2+} cycling in the sarcoplasmic reticulum (SR) (1, 5). The PDE3 inhibitor cilostazol (6–9) and the PDE5 inhibitor sildenafil (10, 11) have been reported to protect hearts against ischemia/reperfusion (I/R) injury in various species. Fukasawa et al. (8) have suggested that cilostazol exerts its cardioprotective effect by activating mitochondrial Ca^{2+}-activated K^+ (mitoK_{Ca}) channels, whose opening protects hearts against infarction (12). Furthermore, studies have shown that the opening of mitoK_{Ca} channels is potentiated by cAMP-dependent PKA signaling (13), whereas PKC potentiates mitochondrial ATP-sensitive K^+ (mitoK_{ATP}) channel activation (14). Kukreja and his associates have suggested that the cardioprotective effects of sildenafil are mediated by activation of both mitoK_{ATP} (10) and mitoK_{Ca} channels (11).

Ischemic preconditioning (PreC), a process in which brief intermittent episodes of ischemia and reperfusion protect the heart from subsequent prolonged ischemic injury (15), initiates a number of cardioprotective signaling pathways at the plasma membrane, which are transduced to mitochondria (16). According to the "signalosome" hypothesis, cardioprotective [e.g., G protein-coupled

Significance

By catalyzing the destruction of cAMP and cGMP, cyclic nucleotide phosphodiesterases (PDEs) regulate their intracellular concentrations and biological actions. Eleven distinct gene families (PDE1–PDE11) define the PDE superfamily. Most families contain several PDE genes. Two separate but related genes generate PDE3 subfamilies PDE3A and PDE3B. Although inhibition of PDE3 protects rodent heart against ischemia/reperfusion (I/R) injury, the specific PDE3 isoform involved is undetermined. Using PDE3A- and PDE3B-KO mice, we report that deletion of PDE3B, but not PDE3A, protected mouse heart from I/R injury in vivo and in vitro, via cAMP-induced preconditioning. To our knowledge, our study is the first to define a role for PDE3B in cardioprotection against I/R injury and suggests PDE3B as a target for cardiovascular therapies.

Author contributions: Y.W.C., C.L., and V.C.M. designed research; Y.W.C., C.L., Y.C., J.S., G.T., F.A., S.G.E., D.H.B., N.P., J.W., and B.S.L. performed research; S.C.H., D.K.R., M.G., and M.P.D. contributed new reagents/analytic tools; Y.W.C., Y.C., J.S., G.T., F.A., S.G.E., D.H.B., N.P., J.W., M.P.D., C.A.B., P.H.B., E.M., and V.C.M. analyzed data; and Y.W.C. and V.C.M. wrote the paper.

The authors declare no conflict of interest.

This article is a PNAS Direct Submission.

[1]Y.W.C. and C.L. contributed equally to this work.

[2]To whom correspondence may be addressed. Email: chungyw@yuhs.ac or manganiv@nhlbi.nih.gov.

This article contains supporting information online at www.pnas.org/lookup/suppl/doi:10.1073/pnas.1416230112/-/DCSupplemental.

receptor (GPCR)-induced or ouabain-induced] signals are delivered to mitochondria by specialized caveolae-derived vesicular structures, signalosomes, which contain a wide variety of receptors (e.g., GPCRs) and signaling molecules (e.g., Akt, Src, eNOS, and PKCε) that are assembled in lipid rafts and caveolae (17). In recent years, the role of lipid rafts and caveolae in cardiovascular signaling has attracted much attention (18), and adenylyl cyclases and PDEs have emerged as key players in shaping and organizing intracellular signaling microdomains (19-21).

Accumulating evidence implicates the mitochondrial permeability transition (MPT) pore as a key effector of cardioprotection against I/R injury, and reperfusion-induced elevation of reactive oxygen species (ROS) can trigger the opening of the MPT pore, resulting in ischemic injury, apoptosis, and cell death (16). A wide range of cardioprotective signaling pathways converge on glycogen synthase kinase-3β (GSK-3β), and its inhibition directly and/or indirectly regulates MPT pore-regulatory factors (e.g., cyclophilin D and voltage-dependent anion channels) and antiapoptotic Bcl-2 family members (22). Physical association between mitochondria and the endoplasmic reticulum (ER) [via mitochondria-associated ER membranes (MAMs)] (23) or the SR (24) also may reduce reperfusion-induced mitochondrial Ca^{2+} overload and consequent oxidative stress and thus block MPT pore opening (25).

In this study, we report that, 24 h after in vivo coronary artery ligation, I/R or, in a Langendorff cardiac I/R model system, infarct size is reduced in PDE3B$^{-/-}$ heart, but not in PDE3A$^{-/-}$ heart, compared with WT heart. This protective effect is most likely caused by reduced production of ROS and reduced Ca^{2+}-induced MPT pore opening in PDE3B$^{-/-}$ mitochondria. The mechanism(s) for cardioprotection in PDE3B$^{-/-}$ mice may be related to cAMP/PKA-induced opening of mitoK_{Ca} channels and assembly of **i**schemia-induced **c**aveolin-3–**e**nriched **f**raction (ICEF) signalosomes in which various cardioprotective molecules accumulate, resulting in functional cardiac preconditioning. Our results also suggest that the increased physical interaction between mitochondria and transverse tubules (T-tubules) (indirectly via the SR at dyads or directly) in PDE3B$^{-/-}$ heart may be involved in ICEF/signalosome delivery of cardioprotective molecules to mitochondria, leading to reduced ROS generation and increased resistance to Ca^{2+}-induced MPT pore opening in PDE3B$^{-/-}$ mitochondria. Although PDE3A is more highly expressed than PDE3B in cardiovascular tissues, our findings of cardioprotection against I/R injury in PDE3B$^{-/-}$ mice but not in PDE3A$^{-/-}$ mice and the different subcellular locations of PDE3A and PDE3B in cardiomyocytes [PDE3A colocalizes with sarco/endoplasmic reticulum Ca^{2+}-ATPase (SERCA) on SR membranes, and PDE3B localizes with caveolin-3 in T-tubules along Z-lines] may reflect an important example of individual PDEs at distinct subcellular sites regulating the compartmentalization of specific cAMP/PKA-signaling pathways (19, 21). In this case, PDE3B, located in regions where cardiomyocyte mitochondria, T-tubules, and SR may be in close proximity, may regulate stress responses and/or the assembly of ICEF signalosomes or other specific cardioprotective pathways.

Results

Targeted Disruption of PDE3B Is Cardioprotective in a cAMP/PKA-Dependent Manner. As shown in Figs. 1 and 2, in vivo coronary artery ligation I/R (Fig. 1) and the Langendorff-perfused heart I/R model (Fig. 2), respectively, were used to investigate the effects of targeted disruption of PDE3B on I/R injury. Compared with WT heart, I/R-related infarct size after in vivo I/R was reduced in PDE3B$^{-/-}$ heart but not in PDE3A$^{-/-}$ heart (Fig. 1 *A*–*C*). Administration of milrinone, a PDE3 inhibitor, to mice before in vivo I/R reduced infarct size in WT and PDE3A$^{-/-}$ hearts but did not further enhance protection in PDE3B$^{-/-}$ mice (Fig. 1 *D* and *E*). As shown in Fig. 2, after in vitro I/R was performed according to the I/R protocol depicted in Fig. 2 *A*, *i*, I/R-induced infarct size also was reduced in Langendorff-perfused PDE3B$^{-/-}$ hearts,

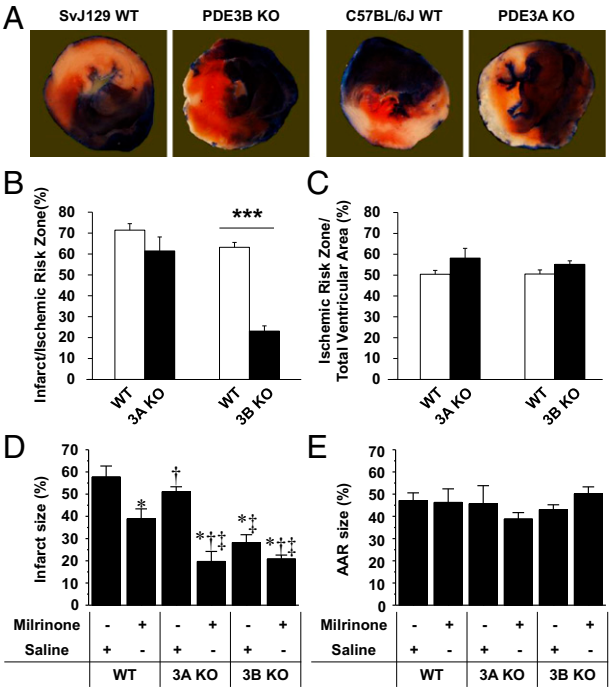

Fig. 1. PDE3B$^{-/-}$ mice, but not PDE3A$^{-/-}$ mice, have smaller infarcts after in vivo coronary artery occlusion/reperfusion, compared with WT mice. Mice were subjected to 30 min of in vivo coronary artery ligation followed by 24-h reperfusion as described in *SI Experimental Procedures*. (*A*) Representative sections of myocardium from WT, PDE3B$^{-/-}$ (3B KO), or PDE3A$^{-/-}$ (3A KO) mice in which I/R-induced myocardial infarction was determined by Evans blue/ triphenyl tetrazolium chloride (TTC) double staining. (*B*) Myocardial infarct size was expressed as a percentage of the infarct area over the ischemic risk zone. (*C*) The size of the ischemic risk zone was expressed as the percentage of ischemic risk zone over total ventricular area. Results are means ± SEM, n = 4–9 animals per group. ***$P < 0.001$ 3B KO vs. WT. (*D* and *E*) Infarct size (*D*) and size of the area at risk (AAR) (*E*) from WT, 3A KO, or 3B KO mice treated with saline or milrinone before I/R, as described in *SI Experimental Procedures*. *$P < 0$ 0.05 vs. WT + saline; †$P < 0.05$ vs. WT + milrinone; ‡$P < 0.05$ vs. 3A KO + saline by one-way ANOVA with Student–Newman–Keul post hoc correction. n = 3–6 animals per group.

compared with WT (Fig. 2 *B* and *C*). Consistent with the reduced infarct size, functional recovery also was increased significantly in PDE3B$^{-/-}$ hearts. As shown in Fig. 2*D*, the rate pressure product (RPP) [RPP = left ventricular developed pressure (LVDP) × heart rate] after 25 min of ischemia and 1.5 h of reperfusion was significantly greater in PDE3B$^{-/-}$ heart than in WT heart, i.e., 56.3 ± 4.5% (n = 8) of preischemic RPP in PDE3B$^{-/-}$ heart compared with only 23.0 ± 4.4% (n = 6) of preischemic RPP in WT heart. As seen in Table S1, hemodynamic parameters measured before and after I/R of Langendorff-perfused hearts from WT, PDE3B$^{-/-}$, and PDE3A$^{-/-}$ mice indicated that the higher RPP in perfused PDE3B$^{-/-}$ hearts after I/R injury was associated with higher LVDP in PDE3B$^{-/-}$ hearts. Consistent with the absence of cardioprotection in vivo (Fig. 1), PDE3A$^{-/-}$ heart did not exhibit improved postischemic recovery in vitro (Fig. 2*E*). Taken together, these results (Figs. 1 and 2) strongly suggest that inhibition of PDE3B, but not of PDE3A, is responsible for the reported cardioprotective effects of PDE3 inhibitors in earlier I/R studies (6–9).

In Western blots, PDE3A was much more highly expressed in heart extracts than in WAT extracts (Fig. S1*A*), whereas PDE3B was more highly expressed in WAT. PDE3B protein was not expressed in either WAT or heart extracts from PDE3B$^{-/-}$ mice. Targeted disruption of PDE3B slightly increased the expression of PDE3A in WAT but not in heart, suggesting that cardioprotection

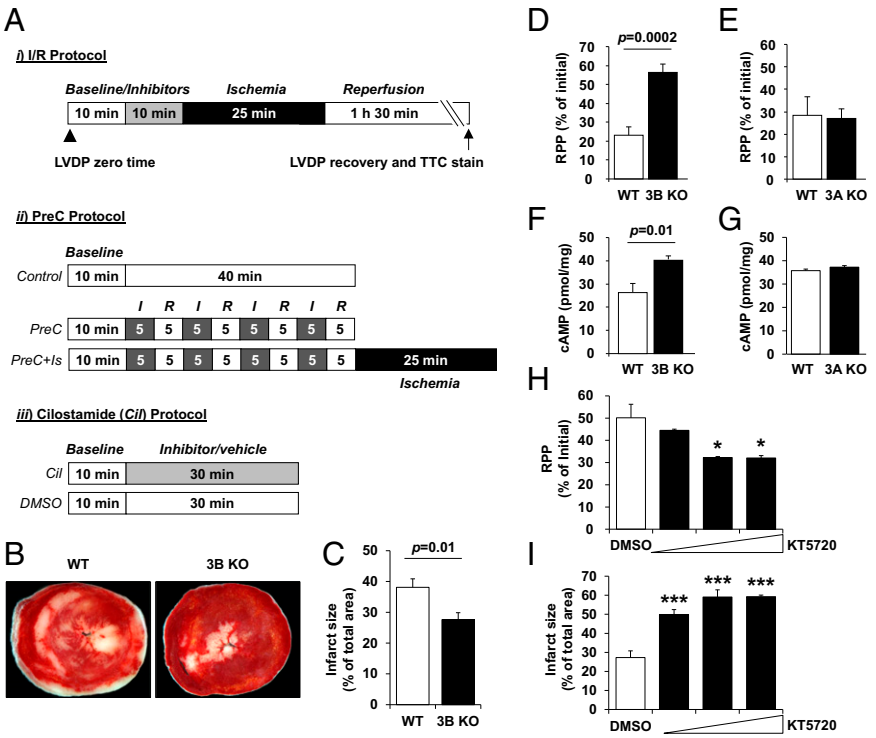

Fig. 2. PDE3B$^{-/-}$-specific cardioprotection against I/R injury is PKA dependent. (*A*) Experimental protocols. Hearts were prepared as described in *SI Experimental Procedures*, and I/R was performed according to the I/R protocol depicted. Initial LVDP was measured at time 0 (arrowhead). The arrow indicates the time point at which postischemic LVDP recovery was measured. Hearts were stained with 1% TTC to analyze infarct size, and I/R samples were collected for further analysis. (*B*) Representative sections of myocardium from WT or PDE3B$^{-/-}$ mice (3B KO), stained with TTC to delineate areas of infarction. (*C*) Infarct size (white areas) is presented as percent of total ventricular area. Results are means ± SEM; $n = 4$–9 animals per group. (*D* and *E*) After I/R (see the I/R protocol in *A*), RPPs of PDE3B$^{-/-}$ (3B KO, male) (*D*) and PDE3A$^{-/-}$ (3A KO, female) (*E*) mice are presented as percent of initial RPP. $n = 4$–8 animals per group. (*F* and *G*) The concentrations of cAMP in PDE3B$^{-/-}$ (*F*) and PDE3A$^{-/-}$ (*G*) hearts were determined as described in *SI Experimental Procedures*. Results are shown as means ± SEM; $n = 7$–20 animals per group. (*H* and *I*), PDE3B$^{-/-}$ hearts were perfused with vehicle (0.1% DMSO) or the PKA inhibitor KT5720 (0.25, 0.5, or 1 μM), according to the I/R protocol depicted in *A*. (*H*) RPP values are expressed as percentages of initial RPP. (*I*) Infarct size is presented as percent of total ventricular area. Results are means ± SEM; *$P < 0.05$; ***$P < 0.001$ vs. DMSO-treated PDE3B$^{-/-}$ by ANOVA. $n = 3$–6 animals per group.

in PDE3B$^{-/-}$ heart was not related to compensatory increased expression of cardiomyocyte PDE3A. Although cAMP was significantly increased in PDE3B$^{-/-}$ heart (Fig. 2*F*), there were no significant changes in either cAMP content (Fig. 2*G*) in PDE3A$^{-/-}$ heart or cGMP content in PDE3B$^{-/-}$ heart (Fig. S2*A*), compared with WT. As indicated in Fig. 2*A*, to study the effects of PKA inhibitor on I/R injury, hearts were perfused with oxygenated buffer containing the PKA inhibitor KT5720 before induction of I/R. As seen in Fig. 2 *H* and *I*, the cardioprotective effect in PDE3B$^{-/-}$ hearts was blocked significantly by KT5720 at concentrations of 0.5 and 1 μM with respect to RPP (Fig. 2*H*) and at 0.25, 0.5, and 1 μM with respect to infarct size (Fig. 2*I*). Consistent with these inhibitory effects of the PKA inhibitor KT5720 (Fig. 2 *H* and *I*) and increased cAMP content (Fig. 2*F*), PKA-induced phosphorylation of several substrates was increased in PDE3B$^{-/-}$ heart (Fig. S1*B*). The observation that cardioprotection in PDE3B$^{-/-}$ heart is PKA dependent is consistent with a prior report which indicated that PKA regulates the opening of the mitoK$_{Ca}$ channel (13) and with the significant inhibition of RPP in PDE3B$^{-/-}$ heart by the mitoK$_{Ca}$ channel inhibitor paxilline (Fig. S2*C*).

Localization of Cardiac PDE3B and PDE3A. We performed cryo-immunogold electron microscopy (EM) to determine where PDE3B and PDE3A are localized in cardiomyocytes. PDE3B-specific labeling was concentrated in the I-band of the sarcomere, consistent with localization to dyads, T-tubules, or the highly elaborated (corbular) SR of the I-band (Fig. 3 *B*–*D*). Caveolin-3, a caveolae protein, is found in both caveolae and T-tubules in heart muscle (26). Double immunogold labeling with PDE3B antibody and caveolin-3 antibody suggested colocalization of the two proteins along the Z-line and on or near T-tubule membranes (Fig. 3*B*), some of which were in contact with mitochondria (Fig. 3*C*). Measurement of the distance between 10-nm gold particles representing caveolin-3 localization and 15-nm particles representing PDE3B localization were consistent with T-tubule localization of PDE3B (Fig. 3*E*). Because deletion of PDE3A did not confer a cardioprotective effect on heart muscle, we suspected that its subcellular distribution might be different from the T-tubule localization of PDE3B. Initial cryo-immunogold EM revealed a distribution of PDE3A immunoreactivity primarily consistent with SR localization. This distribution was confirmed by double cryo-immunogold labeling with antibodies against PDE3A and SERCA2, a marker for the SR (Fig. 3 *F* and *G*). The distribution of immunoreactivity for PDE3A and SERCA2 was highly similar, and they were closely colocalized with a high frequency. This EM localization of PDE3A and SERCA2 is consistent with our recent immunohistochemical localization of murine cardiac PDE3A (27). As seen in Fig. S3, PDE3A colocalized with SERCA2 in PDE3B$^{-/-}$ hearts, as in WT hearts. Fig. 3*H* is a diagrammatic representation of the distribution of PDE3A and PDE3B in WT heart, based on our immunogold labeling results.

PDE3B$^{-/-}$ Cardiac Mitochondria Contact T-Tubules More Frequently and Produce Less ROS. Overexpression of caveolin-3 increases the formation of caveolae and induces cardiac protection by mimicking

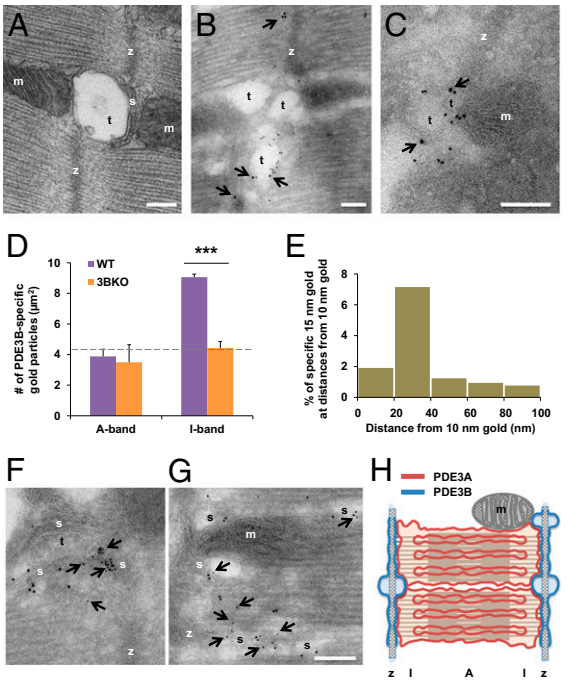

Fig. 3. Different localization of PDE3A and PDE3B in cardiomyocytes. (*A*) Conventional transmission electron microscopy (TEM) images of a longitudinal section of a myocyte showing relationships between T-tubules (t), SR (s), and mitochondria (m) around the Z-line (z). (*B* and *C*) Representative images of immunogold labeling of caveolin-3 (10-nm particles) and PDE3B (15-nm particles, arrows). (*B*) Particles of both sizes are concentrated in the I-band along the Z-line and on or near T-tubule membranes. (*C*) An example of PDE3B labeling close to caveolin-3 labeling on a T-tubule in contact with a mitochondrion. (*D*) The density of 15-nm gold particles (PDE3B) in the A-band and I-band was measured. The dotted line indicates the level of nonspecific labeling. (PDE3B$^{-/-}$ heart muscle was used as a control for nonspecific labeling.) Results are means ± SEM; ***$P < 0.001$ vs. WT. EM images (n = 43–66 per group) were used for counting. (*E*) Histogram showing the frequency of the distance of 15-nm gold particles representing specific PDE3B labeling from the nearest 10-nm particle representing caveolin-3 labeling. The frequency in each range of nonspecific 15-nm gold labeling was subtracted from the total. (*F* and *G*) Representative images of immunogold labeling of SERCA2 (10-nm particles) and PDE3A (5-nm particles, arrows). Particles of both sizes are concentrated on the SR, both at the dyads with T-tubules (*F*) and along the myofibrils and mitochondria (*G*). (*H*) Diagrammatic representation of a cardiac myocyte sarcomere with associated membranous organelles, showing the codistribution of PDE3B with caveolin-3 on T-tubule membranes (blue) along the Z-line and within the I-band (I) and the codistribution of PDE3A with SERCA2 on SR membranes (red) that span the I- and A-band (A). Mitochondria are in close contact with both SR and T-tubules. (Scale bars, 200 nm.)

preconditioning (28). Increased expression of caveolin-3 in cardiac mitochondria was associated with enhanced respiratory function, reduced generation of ROS, and reduced infarct size during in vitro I/R (29). Conversely, caveolin-3$^{-/-}$ mice show very low caveolar density (30) and are resistant to pharmacological preconditioning (31). Given the colocalization of PDE3B with caveolin-3 on or near T-tubule membranes in cardiomyocytes (Fig. 3 *B* and *C*), we examined the location and number of caveolae but were surprised to find no differences in the number of caveolae identified in electron micrographs from WT and PDE3B$^{-/-}$ heart (Fig. S4*A*). Moreover, there was no difference in the number of caveolae in contact with mitochondria close to the sarcolemma. However, as seen in Fig. S4 *A* and *B*, in PDE3B$^{-/-}$ heart there was a small, not statistically significant, increase in the number of T-tubule profiles in contact with category IV mitochondria within the sarcoplasm one myofibril deep from the sarcolemma. There were no significant differences between WT and PDE3B$^{-/-}$ heart in mitochondria numbers (Fig. S4*C*) or in the ratio of mitochondrial DNA (mtDNA) to nuclear DNA (nDNA) (Fig. S4*D*). Because the number of category IV contacts seemed to be greater in PDE3B$^{-/-}$ heart, we counted all contacts between mitochondria and SR/T-tubule junctions (dyads) or directly with T-tubules, areas where PDE3B and caveolin-3 colocalize. These contacts were increased significantly in electron micrographs from PDE3B$^{-/-}$ compared with WT hearts (Fig. 4 *A*–*C*) and perhaps were related to a role for caveolin-3 in the development of the cardioprotective phenotype and signs of preconditioning in PDE3B$^{-/-}$ hearts, including (as described below) reduced ROS (Fig. 4*D*) and increased resistance to Ca^{2+}-induced opening of the MPT pore in the "light" mitochondrial (LM) fraction (Fig. 5*C*) (29).

As described in *SI Experimental Procedures* and shown in Fig. 5*A*, total mitochondria (P2 fractions) were isolated from WT and PDE3B$^{-/-}$ hearts before and after ischemia to assess ROS production. P2 mitochondrial fractions (pellets after centrifugation at 10,000 × g) represent total mitochondria, which include LM and "heavy" mitochondrial (HM) fractions. As shown in Fig. 4*D*, after ischemia, production of ROS was markedly reduced in total mitochondria (P2 fractions) from PDE3B$^{-/-}$ heart, compared with WT mitochondria. These results are consistent with the significant inhibition of RPP in PDE3B$^{-/-}$ heart by the PI3K inhibitor wortmannin (Fig. S2*C*) and with the increased

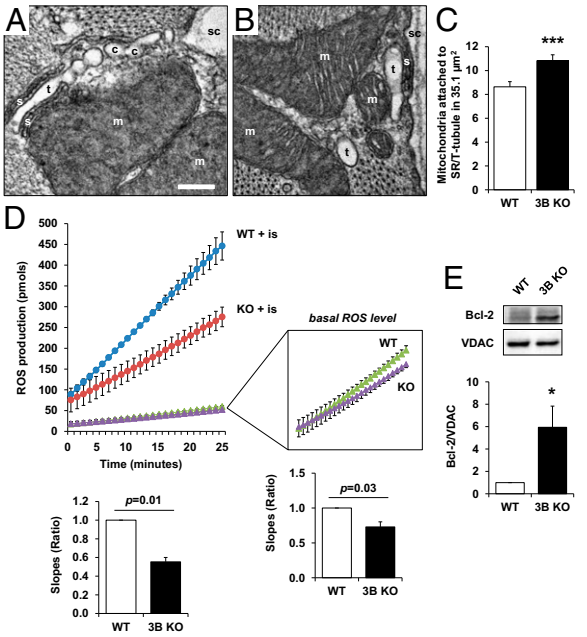

Fig. 4. PDE3B$^{-/-}$ cardiac mitochondria contact T-tubules more frequently and produce less ROS. (*A*–*C*) Conventional TEM images demonstrating interactions between mitochondria, dyad junctions, and T-tubules. (*A* and *B*) Cross-sections of cardiomyocytes near the Z-line. c, caveolae; m, mitochondrion; s, SR; sc, sarcolemma; t, T-tubule. Contacts of mitochondria with dyad junctions (*A*) and directly with T-tubules (*B*) can be seen. (*C*) Average numbers of mitochondria attached to dyad junctions or directly to T-tubules per 35.1 μm^2 of sarcoplasm. EM images (n = 124–127 per group) were used for counting. Results are means ± SEM; ***$P < 0.001$ vs. WT. (Scale bar, 200 nm.) (*D*) As described in *SI Experimental Procedures*, averaged traces of ROS production were measured in the presence of glutamate/malate and ADP by monitoring the oxidation of Amplex Red in WT and PDE3B$^{-/-}$ heart mitochondria fractions isolated after ischemia. Ratios of slopes for rates of ROS production by WT and PDE3B$^{-/-}$ (3B KO) heart mitochondria are presented as bar graphs, with WT as 1. (*Inset*) Basal production of ROS in WT and PDE3B$^{-/-}$ heart mitochondria. n = 3–4 mice per group. (*E*) WT and PDE3B$^{-/-}$ mitochondrial fractions after I/R were used for Western blotting of Bcl-2. The ratio of Bcl-2/voltage-dependent anion channel (VDAC) is mean ± SEM; *$P < 0.05$ vs. WT, n = 4 animals per group.

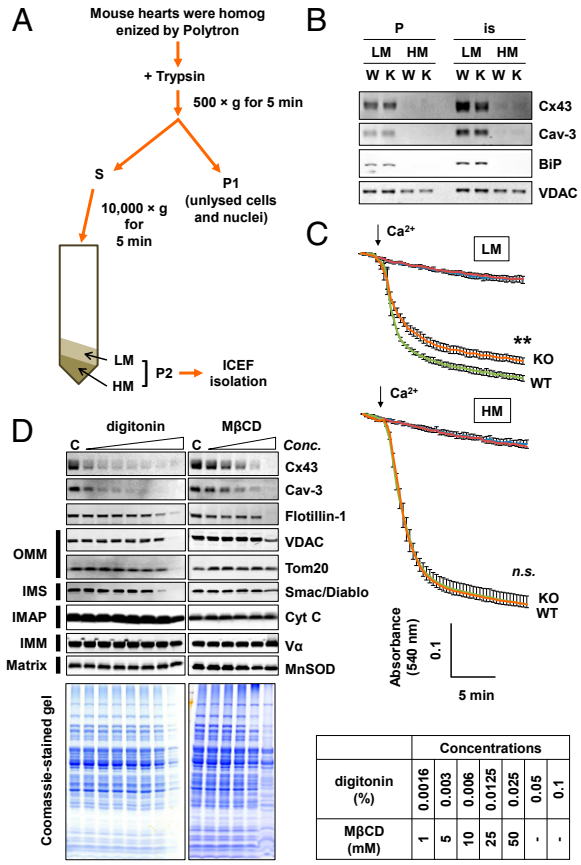

	Concentrations						
digitonin (%)	0.0016	0.003	0.006	0.0125	0.025	0.05	0.1
MβCD (mM)	1	5	10	25	50	-	-

Fig. 5. PDE3B$^{-/-}$ cardiac mitochondrial fractions which contain connexin-43 and caveolin-3 (LM fractions) are more resistant to Ca^{2+}-induced MPT pore opening. (*A*) Schematic representation of procedures for isolation of mitochondrial fractions, as described in *SI Experimental Procedures*. P1, pellet no. 1 after the first spin (500 × *g*); P2, pellet no. 2 after the second spin (10,000 × *g*); S, supernatant after the first spin (500 × *g*). (*B*) As described in *SI Experimental Procedures*, LM and HM fractions were separated from P2 mitochondrial fractions by differential centrifugation. Shown are Western blots of LM and HM fractions isolated from WT (W) and PDE3B$^{-/-}$ (K) hearts before (perfusion only, P) and after (is) ischemia. Western blots (30 μg protein per lane) were performed with antibodies against a gap junction protein connexin-43 (Cx43); caveolin-3 (Cav-3); an ER marker, 78-kDa chaperone BiP/GRP78 (BiP); and a mitochondria marker, VDAC. (*C*) As described in *SI Experimental Procedures*, MPT pore formation was measured as the change in absorbance at 540 nm after stimulation with 400 μM Ca^{2+} (arrow). Results are means ± SEM; $n = 4$–6 animals per group. $^{**}P < 0.01$ vs. WT LM. n.s., not significant. (*D*) Extraction of connexin-43 and caveolin-3 from LM fractions by membrane-disruption assays. (*Upper Left*) As described in *SI Experimental Procedures*, after ischemia, LM fractions were separated from mitochondrial P2 fractions and incubated for 5 min with the cholesterol-removing detergents digitonin (0.002–0.1%) and MβCD (1–50 mM) in serially diluted concentrations, as shown in the table (*Right*). After centrifugation (10,000 × *g*, 5 min), supernatants were discarded, and pellets were analyzed by Western blotting (30 μg protein per lane). c, control; Cav-3, caveolin-3; Cx43, connexin-43; IMAP, inner membrane associated protein; matrix, mitochondrial matrix protein; Vα, ATP synthase (Complex V) subunit α; VDAC, mitochondria marker. (*Lower Left*) Gels were stained with Coomassie blue after transfer. The experiments in *C* and *D* were repeated with 4–6 mice per group.

phosphorylation of Akt and GSK-3β in PDE3B$^{-/-}$ heart (Fig. S2 *D* and *E*). Previous studies have demonstrated that GSK-3β–regulated protection against MPT pore opening is associated with reduced production of ROS (22, 32).

Western blot analysis of heart mitochondrial fractions revealed that antiapoptotic Bcl-2 was increased significantly in PDE3B$^{-/-}$ heart after I/R (Fig. 4*E*). Consistent with these protective changes, phosphorylation of cAMP response element-binding protein (CREB) and expression of the proapoptotic CREB antagonist, inducible cAMP early repressor (ICER) (33), were not elevated in PDE3B$^{-/-}$ heart but were similar to WT (Fig. S1*C*). We previously reported (27) that, compared with WT heart, phosphorylation of CREB, phospholamban, and other substrates of PKA was increased in PDE3A$^{-/-}$ heart, which did not exhibit cardioprotection during I/R (Figs. 1 and 2). As seen in Fig. S1*D*, expression of proapoptotic ICER was increased in PDE3A$^{-/-}$ heart compared with WT heart. Yan et al. (33) have suggested that increased phosphorylation/activation of CREB is an important factor in the up-regulation of ICER expression and subsequent proapoptotic changes (33), which could be a factor in the lack of cardioprotection in PDE3A$^{-/-}$ heart during I/R (Figs. 1 and 2).

Mitochondrial Fractions Isolated from PDE3B$^{-/-}$ Hearts Are More Resistant to Ca^{2+}-Induced MPT Pore Opening. To assess Ca^{2+}-induced swelling, LM and HM fractions were isolated from WT and PDE3B$^{-/-}$ mitochondrial P2 fractions (Fig. 5*A* and *SI Experimental Procedures*) and analyzed by Western blotting (Fig. 5*B*). The LM fraction contained caveolin-3 and connexin-43, which are considered to be subsarcolemmal mitochondria (SSM)-specific proteins (29, 34). Connexin-43 is increased in cardiomyocyte mitochondria during preconditioning (35) and may be critical in protection against myocardial I/R injury (36). LM fractions also contained binding immunoglobulin protein (BiP), an ER marker protein (Fig. 5*B*). The amount of caveolin-3 and connexin-43 in LM fractions increased during ischemia (Fig. 5*B*). As seen in the lower trace in Fig. 5*C*, the HM fraction underwent MPT pore opening as indicated by Ca^{2+}-induced swelling, which resulted in a decrease in absorbance at 540 nm. In general, LM fractions were more resistant than HM fractions to Ca^{2+}-induced swelling. LM fractions from PDE3B$^{-/-}$ heart, however, were significantly more resistant than LM fractions from WT heart (Fig. 5*C*, *Upper*). It is possible that both HM and LM fractions contain SSM, or the LM fraction may be a portion of SSM, which are enriched in caveolin-3 and connexin-43 and are in close proximity to plasma membranes or ER/SR membranes (29). The characteristics of the LM fraction observed here, however, are quite different from those of the SSM described previously (34), especially regarding sensitivity to calcium (Fig. 5*C*) (37).

Because LM fractions were enriched in caveolin-3 and connexin-43, we investigated whether these fractions contained specialized microdomains, such as lipid rafts and caveolae. The location of connexin-43 in LM mitochondria isolated from WT heart after ischemia was examined first by extracting caveolin-3 and connexin-43 from LM mitochondria with proteinase K, as described in a previous study (34), and a nonionic detergent Triton X-100 (TX-100). As shown in Fig. S5, however, these reagents did not allow analysis of differential extraction of caveolin-3 and connexin-43 from specific compartments, because treatment of the LM fraction with proteinase K or TX-100 released caveolin-3 and connexin-43 not only with proteins from the outer membranes of mitochondria (OMM) but also with proteins from the inner membranes of mitochondria (IMM). Because different cellular membranes contain different amounts of cholesterol [which is more abundant in plasma membranes than in the mitochondrial membranes (38)], and caveolae are cholesterol- and sphingolipid-enriched invaginations of the plasma membrane (39), cholesterol-removing detergents such as methyl-β-cyclodextrin (MβCD) or digitonin also were used for extraction of caveolin-3 and connexin-43. As shown in Fig. 5*D*, at concentrations of 25 and 50 mM MβCD, or 0.003–0.025% digitonin, caveolin-3 and connexin-43 were extracted from the LM fraction, accompanied by little or no release of mitochondrial proteins from the OMM or other internal mitochondrial compartments. Although it has been suggested that connexin-43 is located in the IMM (34), these results suggested that connexin-43 might be located in cholesterol-enriched

microdomains, perhaps in caveolin-3–enriched caveolae/signalosomes attached to or in close proximity to the OMM.

Isolation and Proteomic Analysis of ICEFs. To isolate mitochondria-associated caveolae/signalosomes, we modified the well-established isolation methods for caveolae (39) and signalosomes (17). As shown in Fig. 5*A* and Fig. S6*A*, the mitochondrial P2 pellet was fractionated further by stepwise sucrose gradient ultracentrifugation [35, 40, and 45% (wt/vol) sucrose layers] to isolate buoyant fractions, designated as ICEFs. As seen in Fig. S6*B*, ICEFs contained caveolin-1 and caveolin-3, and the caveolin-3 content of ICEFs increased markedly during ischemia.

A comprehensive proteomic characterization of ICEFs isolated from WT and PDE3B$^{-/-}$ hearts before/after ischemia, using isobaric tag for relative and absolute quantification (iTRAQ), identified more than 500 proteins, most of which were mitochondrial (Fig. S6*C*). To identify possible biological pathways in ICEF proteomes, we used the Database for Annotation, Visualization and Integrated Discovery (DAVID) 6.7 tool to analyze Kyoto Encyclopedia of Genes and Genomes (KEGG) pathways. Although only the cardiac muscle contraction pathway was enriched in the top 10 pathways, three other cardiac function-related pathways also were enriched significantly: arrhythmogenic right ventricular cardiomyopathy, dilated cardiomyopathy, and hypertrophic cardiomyopathy (Fig. S6*D*).

Table S2 lists 57 ICEF proteins in which at least one of three ratios was significantly different: (*i*) between PDE3B$^{-/-}$ and WT before ischemia (KO/WT); (*ii*) between WT after ischemia and WT before ischemia (WT+is/WT); and (*iii*) between PDE3B$^{-/-}$ after ischemia and PDE3B$^{-/-}$ before ischemia (KO+is/KO). Interestingly, as seen in Fig. 6*A*, the ICEF proteome contains three components of dysferlin-mediated membrane repair machinery (40), i.e., dysferlin, annexin A2, and the newly described tripartite motif family protein (TRIM72) (41), as well as calcium-signaling proteins, SERCA2, calnexin, calsequestrin-2, cadherin-13, and sarcalumenin (Fig. S7). The iTRAQ results (Fig. 6*A* and Table S2) indicated that, compared with ICEFs in WT heart, many of these proteins were significantly enriched in ICEFs of PDE3B$^{-/-}$ heart before ischemia and increased further in ICEFs of WT heart during ischemia; this finding is consistent with the idea that PDE3B$^{-/-}$ heart might be functionally preconditioned. The ICEF proteome also contains seven proteins (nos. 3, 6, 32, 34, 44, 46, and 47 in Fig. 6*A* and Table S2), thought to be possibly cardioprotective and found in a larger group of proteins identified in a mitochondrial proteomic profile induced during the exposure of perfused hearts to the GSK inhibitor SB216763 (42).

Western blot analysis confirmed that TRIM72 protein was significantly enriched in ICEFs of PDE3B$^{-/-}$ heart before ischemia (Fig. 6 *B* and *C*). Although caveolin-3 and connexin-43 were not detected by iTRAQ, Western blots indicated that their protein expression before ischemia, like that of TRIM72, was increased in PDE3B$^{-/-}$ ICEFs compared with WT ICEFs (Fig. 6*B*, *Left*). TRIM72, caveolin-3, and connexin-43 also were increased in ICEFs during preconditioning of WT hearts (Fig. 6*B*, *Right*). Accumulation of caveolin-3 and connexin-43 in ICEFs increased further during ischemia and to a greater extent than TRIM72 (Fig. 6*B*, *Left*, and Fig. 6*C*). Furthermore, as seen in Fig. 6 *D* and *E*, exposure to the PKA inhibitor KT5720 largely blocked the accumulation of these proteins in PDE3B$^{-/-}$ ICEFs during ischemia, whereas the PKG inhibitor KT5823 and the P13K inhibitor wortmannin did not, suggesting that ICEF assembly is PKA dependent. As shown in Fig. 6*F*, a similar accumulation of these proteins was observed in the ICEFs of cilostamide-treated WT hearts after perfused hearts were incubated with the potent PDE3 inhibitor cilostamide according to the cilostamide inhibitor protocol in Fig. 2*A*.

Functional annotation with Gene Ontology (GO), using the DAVID functional annotation tool (david.abcc.ncifcrf.gov)

A

No.	Identified Proteins	KO / WT	WT+is / WT	KO+is / KO	n	Related Pathways	Ref
4	Annexin A2	1.30 ± 0.12†	1.39 ± 0.16†	1.04 ± 0.10	6	Dysferlin-mediated membrane repair machinery	40,41
20	Dysferlin	1.38 ± 0.12*	1.47 ± 0.16	1.06 ± 0.06	4		
57	Tripartite motif-containing protein 72	1.53 ± 0.14*	1.63 ± 0.18*	0.98 ± 0.10	4		
3	Fructose-bisphosphate aldolase A	1.15 ± 0.08	1.70 ± 0.17*	1.47 ± 0.12**	6	GSK-dependent cardioprotection (mitochondrial)	42
6	Annexin A6	1.32 ± 0.13	2.09 ± 0.31*	1.31 ± 0.22	6		
32	Heat shock protein HSP 90-beta	1.26 ± 0.10	1.71 ± 0.20*	1.33 ± 0.11*	6		
34	Heat shock cognate 71 kDa protein	1.29 ± 0.10*	1.70 ± 0.27*	1.42 ± 0.11*	6		
44	6-phosphofructokinase, muscle type	1.08 ± 0.07	1.51 ± 0.16*	1.37 ± 0.13*	6		
46	Phosphoglycerate kinase 1	0.95 ± 0.06	1.11 ± 0.13	1.57 ± 0.03***	4		
47	Pyruvate kinase isozymes M1/M2	1.45 ± 0.09	2.37 ± 0.27*	1.62 ± 0.12**	6		

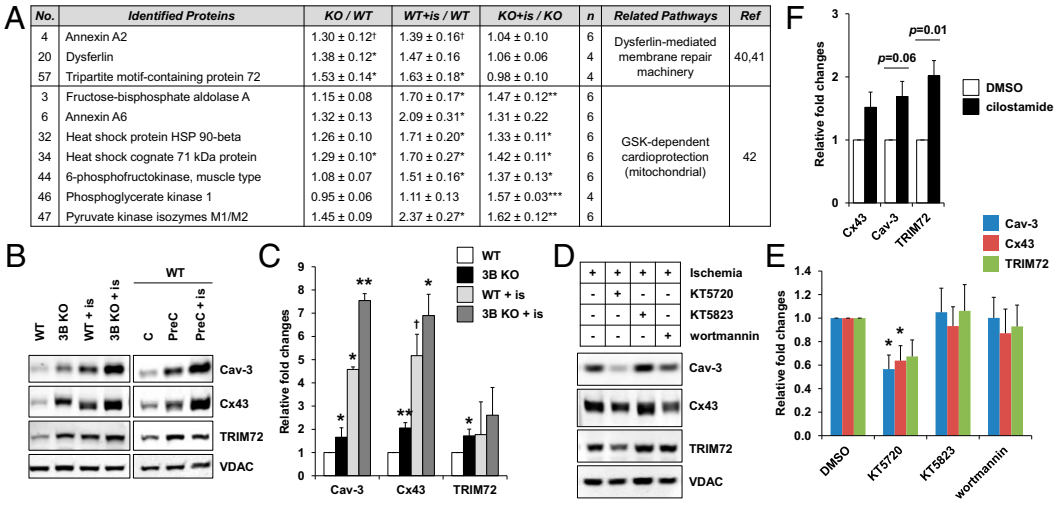

Fig. 6. Accumulation of proteins into ICEFs is PKA dependent. (*A*) Representative list of protective proteins (components of membrane-repair machinery and proteins in the mitochondrial fraction increased during treatment with a GSK inhibitor) among the 57 ICEF proteins selected by $P < 0.06$, with relative fold changes compared by iTRAQ between WT and PDE3B KO cells before and after (+is) ischemia. Values are normalized by an average of VDAC-1, VDAC-2, and VDAC-3. Results are means ± SEM. $^{\dagger}P < 0.06$; $^{*}P < 0.05$; $^{**}P < 0.01$; $^{***}P < 0.001$. *n* = number of independent experiments. The 57 proteins are listed in Table S2. (*B*, *Left*) Representative Western blots of ICEFs isolated from WT and PDE3B$^{-/-}$ heart before and after (+Is) ischemia for 25 min according to the I/R protocol (no reperfusion) depicted in Fig. 2*A*. (*Right*) ICEFs isolated from WT hearts either after preconditioning (PreC) or after preconditioning followed by ischemia (PreC + Is) according to the PreC protocol depicted in Fig. 2*A*. (*C*) Bar graphs showing relative changes in several ICEF proteins in WT and PDE3B$^{-/-}$ hearts before and after ischemia (Is) (*B*, *Left*). Results are means ± SEM. $^{*}P < 0.05$; $^{\dagger}P < 0.06$; $^{**}P < 0.01$ vs. WT before ischemia. (*D*) Western blots of ICEFs isolated from PDE3B$^{-/-}$ hearts perfused in the presence of 1 μM KT5720, 1 μM KT5823, or 100 nM wortmannin, followed by ischemia for 25 min according to the I/R protocol (no reperfusion) depicted in Fig. 2*A*. (*E*) Fold changes are shown as means ± SEM. $^{*}P < 0.05$ vs. DMSO. (*F*) ICEFs were isolated from WT hearts after perfusion with the selective PDE3 inhibitor cilostamide (1 μM) for 30 min according to the cilostamide protocol depicted in Fig. 2*A*. Western blots in *B* and *D* (30 μg protein per lane) were incubated with antibodies against caveolin-3, connexin-43, TRIM72, and VDAC. In *C*, *E*, and *F*, the intensity of blots is presented as relative fold changes normalized by the intensity of VDAC. Results are means ± SEM; *n* = 4–9 animals per group.

suggested that the differentially accumulated proteins in ICEFs could be divided into three categories of GO annotations: cellular component, molecular function, and biological process (Table S3). To identify the underlying biological function further, the differentially accumulated 57 ICEF proteins were imported into the Cytoscape tool. Then GO analysis was performed with the BiNGO tool (Fig. S8*A*). It was of interest that we found Z disk and I band of subcluster no. 2 (sarcomere), which are linked to subcluster no. 1 (mitochondria) via subcluster no. 3 (organelle), suggesting an ICEF-mediated interaction between mitochondria and sarcomeres (Z disk and I band). Consistent with EM data (Figs. 3 and 4 *A* and *B*) and iTRAQ data, Western blots indicated that the SR marker protein calsequestrin was highly enriched in ICEFs from PDE3B$^{-/-}$ heart (compared with WT heart) together with T-tubule L-type Ca^{2+} channel ($Ca_V1.2$) (Fig. S8 *B–D*). During ischemia, accumulation of Cav 1.2 and calsequestrin in ICEFs, similar to that of TRIM72 (Fig. 6*D*), was blocked by the PKA inhibitor KT5720 but not by the PI3K inhibitor wortmannin or the PKG inhibitor KT5823 (Fig. S8*E*).

Discussion

Studies with PDE3A$^{-/-}$ and PDE3B$^{-/-}$ mice have been informative in delineating specific functional roles for PDE3A and PDE3B isoforms that may be relevant to human physiological and pathophysiological processes. PDE3A, for example, regulates platelet aggregation and basal myocardial contractility (43), as well as cell-cycle progression in oocytes [female PDE3A$^{-/-}$mice, but not female PDE3B$^{-/-}$ mice, are infertile (3)] and murine vascular smooth muscle cells (44). This latter work supports a possible role for PDE3A, but not for PDE3B, in modulating poststenting or postangioplasty vascular remodeling and suggests that the inhibition of PDE3A mediates some of the reported beneficial effects of cilostazol, a PDE3 inhibitor, in reducing poststenting restenosis and progression of carotid intima-media thickness in some patients (45, 46). Earlier work with PDE3B$^{-/-}$ mice suggested that PDE3B regulates energy metabolism (4), and we recently reported that in PDE3B KO mice WAT assumes phenotypic characteristics of BAT (47).

The results presented here with PDE3B$^{-/-}$ mice strongly suggest that PDE3B is the isoform responsible for the cardioprotective effects against I/R injury associated with the pharmacological inhibition of PDE3 (6–9). These studies also indicate, for the first time to our knowledge, distinct subcellular locations of PDE3A and PDE3B in cardiomyocytes, with PDE3A distributed with SERCA2 on SR membranes and PDE3B colocalizing with caveolin-3 along the Z-line and on or near T-tubule membranes, close to mitochondria (Fig. 3*B*). PDE3B may be a unique PDE in these areas, where it may play an important role in regulating compartmentalized cAMP-signaling pathways (1, 19, 21, 48, 49). The observation that cAMP is increased in PDE3B$^{-/-}$hearts but not in PDE3A$^{-/-}$hearts (Fig. 2 *F* and *G*) suggests that PDE3B may regulate a pool of cAMP that is not readily accessed by other PDEs. However PDE3A may share compartments with other PDEs, especially PDE4 (50, 51). For example, PDE3A, PDE4A, and PDE4B are recruited to PI3Kγ- and PKA-based multimolecular complexes in murine cardiomyocytes. In these complexes they are activated by PKA and thereby block, in a feed-back fashion, cAMP/PKA-initiated and Ca^{2+}-dependent ventricular arrhythmias; these PDEs could exist in the same compartment or in unique or functionally overlapping ones (51).

The increased cAMP (Fig. 2*F*) and phosphorylation of several PKA substrates (but not CREB) (Fig. S1 *B* and *C*), as well as the inhibitory effects of the PKA inhibitor KT5720 on RPP (Fig. 2*H*), infarct size (Fig. 2*I*), and assembly of ICEF signalosomes (Fig. 6*D* and Fig. S8*E*), in PBE3B$^{-/-}$ heart, suggest that cardioprotection may be regulated via compartmentalized cAMP/PKA-signaling pathways. The increase in cAMP content and activation of PKA may enhance the assembly of ICEF/signalosomes and localized PKA-dependent opening of mitoK$_{Ca}$ channels (Fig. S2*C*, paxilline) and thereby protect the PDE3B$^{-/-}$heart from I/R injury. Compared with WT, PDE3B$^{-/-}$ cardiac mitochondria fractions are preconditioned, in that they contain more cardioprotective ICEF proteins, produce less ROS, and are more resistant to Ca^{2+}-induced MPT pore opening.

We cannot exclude the possibility that cGMP/PKG-signaling pathways also are involved in cardioprotective mechanisms in PDE3B$^{-/-}$ mice in a manner that suggests cAMP- and cGMP-signaling cross talk. The significant inhibition of RPP in PDE3B$^{-/-}$ heart by the PI3K inhibitor wortmannin and the PKG inhibitor KT5823 [by 52.4% and 35.3%, respectively, compared with DMSO (Fig. S2*C*)] suggested that cardioprotection also may be regulated via PI3K/Akt/eNOS/PKG-signaling pathways, in which cGMP and nitric oxide might play an important role, or the PI3K/Akt/GSK-3β pathway, which also is known as the "reperfusion injury salvage kinase" pathway (16). Because the eNOS inhibitor L-NG-nitro-arginine methyl ester (L-NAME) did not block the beneficial effect of PDE3B ablation on RPP (Fig. S2*B*), and no changes in cGMP levels (Fig. S2*A*) or in phosphorylation of eNOS by Western blot analysis (Fig. S2*F*) were observed, the case for the PI3K/Akt/GSK-3β pathway seems more convincing. This notion was supported by the increased level of phosphorylated Akt (Fig. S2*D*) and phosphorylated GSK-3β (Fig. S2*E*) in PDE3B$^{-/-}$ heart and is consistent with published results of others (52) which indicated that, during preconditioning, GSK-3β was phosphorylated and inhibited in a wortmannin-sensitive manner. GSK-3β is an integration point of various cardioprotective signaling pathways which ultimately prevent MPT pore opening (22). A role for phosphorylated GSK-3β in cardioprotection of PDE3B$^{-/-}$ heart also is supported by the increased expression of antiapoptotic Bcl2 (Fig. 4*E*) and the PDE3B$^{-/-}$ ICEF proteome, which includes proteins that are induced by inhibition of GSK-3β (Fig. 6*A* and Table S2) and are thought to be cardioprotective (42). It is of interest that phosphorylation of GSK-3β and up-regulation of Bcl-2 also were observed in I/R hearts perfused with the PDE5 inhibitor sildenafil (53), and it has been further suggested that the cardioprotective effects of sildenafil are mediated by activation of both mitoK$_{ATP}$ (10) and mitoK$_{Ca}$ channels (11).

Interestingly, the association of four ICEF proteins [fructose-bisphosphate aldolase A, annexin A6, heat-shock cognate 71 kDa protein (HSC70), and pyruvate kinase isozymes M1/M2] with mitochondria also was reported to be blocked significantly by the heat-shock protein 90 (HSP90) inhibitor geldanamycin (42), suggesting that at least some ICEF proteins may be transported into mitochondria via the HSC70-HSP90-TOM70 system (HSC70 and HSP90 are found in ICEFs) (54). It also has been suggested that mitochondrial connexin-43 translocates to IMM through the HSP90-dependent translocase complex of the outer mitochondrial membrane (TOM) pathway (36) and plays a crucial role in cardioprotection associated with the PI3K/Akt/GSK-3β pathways (55). In PDE3B$^{-/-}$ heart the improved postischemic recovery of RPP was inhibited significantly by blocking the PKA-dependent mitoK$_{Ca}$ channel opening by paxilline (Fig. S2*C*). This observation was consistent with the reported effects of cilostazol on the PKA-regulated mitoK$_{Ca}$ channel (8) but not with mitoK$_{ATP}$ channel blocking by 5-hydroxydecanoic acid (5-HD), which is PKG/PKC dependent (Fig. S2*C*). The results of our studies with paxilline and 5-HD, which suggest that cardioprotection may be related to cAMP/PKA-induced activation of the mitoK$_{Ca}$ channel, are consistent with other studies discussed in this report, i.e., the effects of PKA and PKG inhibitors (Figs. 2 *H* and *I* and 6*D* and Figs. S2*C* and S8*E*) and the effects of the PDE3 inhibitor cilostamide (Fig. 6*F*). However, because paxilline and 5-HD (or other pharmacological agents) are not completely specific for ion channels (or other targets), interpretation of studies that use pharmacological agents should be tempered by the possibility of off-target effects and responses. To understand better

the cardioprotective mechanisms in PDE3B$^{-/-}$ heart, more studies will be required to identify specific target protein(s) of PKA and a possible role for PKG in cAMP/cGMP cross talk, as well as to define the precise localization and functional role of connexin-43 in ICEFs.

In membrane repair machinery dynamics, TRIM72 is thought to interact physically with dysferlin and caveolin-3 and to translocate them to sites of membrane damage (41). Recently it has been demonstrated that I/R reduces the protein level of TRIM72 and that preconditioning prevents I/R-induced down-regulation of TRIM72 (56). In addition, I/R-induced mitochondrial dysfunction and cardiomyocyte death were exacerbated in TRIM72-deficient mice (57). Therefore, the increased amount of TRIM72 in PDE3B$^{-/-}$ ICEFs (Fig. 6 and Table S2) is consistent with the idea that the PDE3B$^{-/-}$ heart is preconditioned. Although the involvement of mitochondria in TRIM72-mediated cardioprotection is not certain, our findings suggest that ICEF signalosomes may be a specialized microdomain that delivers membrane repair machinery to damaged mitochondrial membranes. The increased amount of TRIM72 in PDE3B$^{-/-}$ ICEFs and the accumulation of TRIM72 in ICEFs during perfusion in the presence of the PDE3 inhibitor cilostamide support the notion that selective inhibition of myocardial PDE3B might provide a novel cardioprotective therapeutic strategy for the treatment of ischemic injury and myocardial infarction.

Caveolin-3 is a skeletal, cardiac, and smooth muscle-specific isoform of caveolin, a protein marker for caveolae. Although recognized as cholesterol- and sphingolipid-enriched 50- to 100-nm invaginations of the plasma membrane (18, 39, 58), caveolae also are found in non-plasma membrane locations (e.g., developing T-tubules) (59). Although no significant changes in the number of caveolae and mitochondria were observed between WT and PDE3B$^{-/-}$ heart, more mitochondria in PDE3B$^{-/-}$ heart were in contact with T-tubules or T-tubule/SR dyads (Fig. 4 *A* and *B*), whose T-tubule membranes are derived from and are continuous with caveolae (Fig. 4*A*). During ischemia, the amount of caveolin-3, which colocalizes with PDE3B, increases in LM fractions (Fig. 5*B*) and is incorporated into ICEFs (Fig. 6*B* and Fig. S6*B*). Taken together, the increased amount of $Ca_V1.2$ and calsequestrin in PDE3B$^{-/-}$ ICEFs (Fig. S8 *B–D*), the increased number of contacts between mitochondria and T-tubules or dyads (Fig. 4*C*), and the localization of PDE3B on or near T-tubules (Fig. 3 *B–E*) suggest mechanisms, perhaps similar to preconditioning, whereby compartmentalized cardioprotective signaling molecules in caveolae/signalosomes translocate to PDE3B$^{-/-}$ mitochondria, resulting in reduced Ca^{2+} overload and reduced MPT pore opening (16).

cAMP-signaling pathways are highly compartmentalized, and PDEs play an important role in this compartmentalization (1, 19, 21, 48, 49). Individual PDEs are targeted to or tethered at different subcellular locations where they are incorporated, via protein/protein interactions, into macromolecular signaling complexes. In these microdomains they regulate compartment-restricted cAMP gradients and specific cAMP-signaling pathways and, thereby, specific biological processes (19, 21, 48, 49). Using PDE3A$^{-/-}$ and PDE3B$^{-/-}$ mice, we found that PDE3A, not PDE3B, regulates basal myocardial contractility (27, 43). PDE3A, as a component of an SERCA2 multimolecular regulatory complex, modulates myocardial contractility by regulating cAMP-mediated phosphorylation of phospholamban, activation of SERCA2, and uptake of Ca^{2+} into the SR (27). Our recent findings indicate that human PDE3A is a component of a similar SERCA2 regulatory complex in human myocardium (60). In adipocytes, PDE3B also is recruited to localized multimolecular complexes that regulate insulin and cAMP/PKA-signaling pathways (61, 62).

In this regard, PI3Kγ is a multifunctional protein, which has been shown to serve as a link between cAMP/PKA- and phosphatidylinositol(3,4,5)-triphosphate (PIP_3)-signaling pathways (63–65). Specifically, in isolated murine ventricular myocytes, PI3Kγ seems to be an important regulator of PDE4 activity and its function in modulating cAMP-induced Ca^{2+} transients, uptake of Ca^{2+} via SERCA2 into the sarco/endoplasmic reticulum (SER), and, consequently, enhancing myocardial contractility (50). PI3Kγ also serves as an A-kinase anchor protein (AKAP)/scaffolding protein which recruits PDE3A, PDE4A and PDE4B (but not PDE4D), and PKA to localized multimolecular complexes in isolated murine ventricular myocytes (51). In these distinct complexes, cAMP/PKA-induced phosphorylation/activation of these different PDEs initiated a negative feedback loop which decreased cAMP/PKA-induced phosphorylation of L-type calcium channels and phospholamban and thus prevented cAMP-dependent, calcium-induced ventricular arrhythmias (51).

PI3Kγ also recruited PDE3B to a multimolecular complex containing the PI3Kγ p84/p87/p110γ heterodimer, PKA, and PDE3B (64, 65). In this complex, PKA phosphorylates/activates PDE3B and phosphorylates PI3Kγ, thus inhibiting its kinase activity and blocking its proinflammatory effects (64, 65). Through mechanisms independent of its kinase activity but apparently dependent on its function as an AKAP/scaffolding protein in the PI3Kγ/PKA/PDE3B multimolecular complex, PI3Kγ was hypothesized to protect against cardiac damage produced by pressure overload induced by transaortic constriction via regulation of PKA-induced activation of PDE3B and cAMP turnover, maintenance of β-adrenergic receptor density on the cell surface, and enhancement of myocardial function and contractility (64, 65, 66). It is possible that in PDE3B$^{-/-}$ heart the absence of PDE3B in the PI3Kγ/PKA/PDE3B complex leads to increased cAMP/PKA signaling (Fig. 2*F* and Fig. S1*B*) and increased phosphorylation and inhibition of PI3Kγ activity, with decreased production of proinflammatory signals. At this point, however, the detailed mechanisms for the integration of the activated cAMP/PKA-signaling pathways and the kinase-dependent and -independent actions of PI3Kγ on the development of the cardioprotective phenotype require further investigation. Although PI3Kγ regulates multiple PDEs, the molecular mechanisms for regulation remain largely unknown and seem to differ in different cells and tissues. This variability is not surprising, because PDEs in different cells subsume different roles and associate with different multimolecular complexes.

Taken together, our observations are consistent with a model in which differentially localized PDE3A and PDE3B enzymes regulate cAMP compartmentalization and/or Ca^{2+} transients within microdomains in the SR that contain PDE3A, SERCA2, and phospholamban (27) or within microdomains in the sarcomere that contain PDE3B, $Ca_V1.2$, and calsequestrin and are located where T-tubules, SR, and mitochondria are in close proximity and, most likely, interact and cross talk (Figs. 3 and 4) (1, 19, 21, 48, 49). PDE3B is relatively highly expressed in tissues important in the regulation of energy homeostasis (2). Our earlier studies with adipose tissue from PDE3B$^{-/-}$ mice suggested that PDE3B regulates energy metabolism (4) and that, in PDE3B$^{-/-}$mice, WAT assumed phenotypic characteristics of BAT, including increased mitochondrial biogenesis, oxygen consumption and fatty acid oxidation, and increased expression of uncoupling protein-1 (47). Given its location (Figs. 3 and 4), PDE3B may be a component of MAMs involved in integrating Ca^{2+} signaling between mitochondria and SER (23, 24). As in adipose tissue (47), perhaps PDE3B deletion alters cardiomyocyte energetics and thus protects the heart from ischemic insult.

We also have suggested that PDE3A, not PDE3B, is the most likely target of PDE3 inhibitors (e.g., milrinone) that enhance myocardial contractility (27, 43). However, although the PDE3 inhibitor cilostazol is used for treating intermittent claudication, a peripheral vascular disease (67), chronic administration of the PDE3 inhibitor milrinone as therapy for heart failure was associated with an increase in the incidence of ventricular arrhythmias and mortality (68). Yan et al. (33) have suggested that one possible mechanism for the untoward effects of chronic inhibition of

myocardial PDE3, especially PDE3A, by milrinone might involve phospho-CREB–induced expression of ICER and subsequent apoptosis and myocardial pathological remodeling. Consistent with these findings, Oikawa et al. (69) recently have reported that specific overexpression of myocardial PDE3A1 in transgenic mice confers protection during I/R by decreasing cAMP signaling and phosphorylation of CREB, resulting in decreased expression of ICER and reduced apoptosis during I/R. Taken together, this report and our data suggest that differentially localized PDE3A and PDE3B modulate I/R injury, perhaps via different but overlapping mechanisms in distinct compartments (Figs. 3 and 4). We suggest that PDE3B deletion/inhibition confers cardioprotective effects during I/R, most likely through cAMP/PKA-induced preconditioning, which is associated with the accumulation of proteins with cardioprotective function in ICEFs, resulting in enhanced PKA-dependent opening of mitoK$_{Ca}$ channels, reduced generation of ROS, and inhibition of MPT pore opening. In another compartment, activation/increased expression of PDE3A would confer protection via inhibition of cAMP signaling, ICER expression, and apoptosis.

Our current and previously published data (27, 43, 44, 60) and that of Yan and coworkers (33, 69) also clearly point out the need for, problems with, and therapeutic promise of inhibitors that selectively target localized PDE3 isoforms. Currently available PDE3 inhibitors have little or no selectivity for PDE3A versus PDE3B, because the catalytic domains of PDE3A and PDE3B are very similar. In mice with type 2 diabetes, cilostazol enhanced the ability of exenatide and a dipeptidyl-peptidase-4 inhibitor to limit the extent of IR injury (70, 71). Given these reports and our findings of cardioprotection in PDE3B$^{-/-}$ mice, PDE3B-selective inhibitors might provide benefit in heart transplant patients and heart failure patients, and perhaps in type 2 diabetics, by limiting I/R damage. The case for PDE3A inhibitors, which enhance contractility but also may increase apoptosis and pathological remodeling in cardiomyocytes, is much more complex. Three isoforms generated from the single PDE3A gene— PDE3A1, PDE3A2, and PDE3A3—have been identified (72). These isoforms possess identical amino acid sequences except for the deletion of different lengths of the N-terminal region, and the recombinant (r) PDE3A1, rPDE3A2, and rPDE3A3 isoforms exhibit virtually identical catalytic properties and inhibitor sensitivities (73). Selective inhibition of PDE3A isoforms that are incorporated into the SERCA2 regulatory complex described above or blocking the integration of PDE3A into these SERCA2-containing complexes might enhance contractility and provide therapy for heart failure without the harmful effects of increased apoptosis and pathological remodeling that might accompany diffuse increases in intracellular cAMP content in other compartments that arise from global inhibition of PDE3A isoforms. Although it is tempting to draw connections and speculate about the role of PDE3A in human cardiovascular physiology and pathophysiology, it is less justified to do so regarding PDE3B, because less is known about its location and function in human heart.

In summary, in this study we isolated, identified, and characterized ICEFs/signalosomes in mouse heart mitochondrial fractions and suggested their importance in physiological regulation of cardioprotection in PDE3B$^{-/-}$ heart. Importantly, we demonstrated, for the first time to our knowledge, that ICEFs may be mitochondria-specific signalosomes that share characteristics of signalosomes isolated from heart homogenates by conventional methods (17) and contain cardioprotective proteins, including connexin-43, several calcium-signaling proteins (Fig. S7), and membrane repair machinery (40), including recently described TRIM72 (Fig. 6*F*) (56, 57). Further study is required to understand mechanisms for preconditioning in PDE3B$^{-/-}$ heart, how PKA regulates ICEF assembly, and how cardioprotective signaling molecules in ICEFs are transferred to mitochondria and activate mitoK$_{Ca}$ channels and other cardioprotective events.

Experimental Procedures

Animals. PDE3A$^{-/-}$ and PDE3B$^{-/-}$ mice were generated as previously described (3, 4). Protocols for mouse generation and maintenance and all animal studies were approved by the National Heart, Lung, and Blood Institute Animal Care and Use Committee (Protocol H-0024).

Statistical Analysis. Data are expressed as mean ± SEM. Student's *t* test or one-way ANOVA were used for comparison of groups. Values of *P* less than 0.05 were considered statistically significant.

Further details are given in *SI Experimental Procedures*.

ACKNOWLEDGMENTS. We thank Dr. M. Movsesian of the University of Utah School of Medicine for helpful discussions. Y.W.C., C.L., Y.C., J.S., G.T., S.C.H., F.A., S.G.E., D.H.B., D.K.R., M.G., M.P.D., E.M., and V.C.M. were supported by the National Heart, Lung, and Blood Institute Intramural Research Program. N.P., J.W., and P.H.B. were supported by Canadian Institutes for Health Research Grant MOP62954.

1. Zaccolo M, Movsesian MA (2007) cAMP and cGMP signaling cross-talk: Role of phosphodiesterases and implications for cardiac pathophysiology. *Circ Res* 100(11):1569–1578.
2. Shakur Y, et al. (2001) Regulation and function of the cyclic nucleotide phosphodiesterase (PDE3) gene family. *Prog Nucleic Acid Res Mol Biol* 66:241–277.
3. Masciarelli S, et al. (2004) Cyclic nucleotide phosphodiesterase 3A-deficient mice as a model of female infertility. *J Clin Invest* 114(2):196–205.
4. Choi YH, et al. (2006) Alterations in regulation of energy homeostasis in cyclic nucleotide phosphodiesterase 3B-null mice. *J Clin Invest* 116(12):3240–3251.
5. Shakur Y, et al. (2002) Comparison of the effects of cilostazol and milrinone on cAMP-PDE activity, intracellular cAMP and calcium in the heart. *Cardiovasc Drugs Ther* 16(5):417–427.
6. Sanada S, et al. (2001) Cardioprotective effect afforded by transient exposure to phosphodiesterase III inhibitors: The role of protein kinase A and p38 mitogen-activated protein kinase. *Circulation* 104(6):705–710.
7. Manickavasagam S, et al. (2007) The cardioprotective effect of a statin and cilostazol combination: Relationship to Akt and endothelial nitric oxide synthase activation. *Cardiovasc Drugs Ther* 21(5):321–330.
8. Fukasawa M, Nishida H, Sato T, Miyazaki M, Nakaya H (2008) 6-[4-(1-Cyclohexyl-1H-tetrazol-5-yl)butoxy]-3,4-dihydro-2-(1H)quinolinone (cilostazol), a phosphodiesterase type 3 inhibitor, reduces infarct size via activation of mitochondrial Ca2+-activated K+ channels in rabbit hearts. *J Pharmacol Exp Ther* 326(1):100–104.
9. Tosaka S, et al. (2007) Cardioprotection induced by olprinone, a phosphodiesterase III inhibitor, involves phosphatidylinositol-3-OH kinase-Akt and a mitochondrial permeability transition pore during early reperfusion. *J Anesth* 21(2):176–180.
10. Ockaili R, Salloum F, Hawkins J, Kukreja RC (2002) Sildenafil (Viagra) induces powerful cardioprotective effect via opening of mitochondrial K(ATP) channels in rabbits. *Am J Physiol Heart Circ Physiol* 283(3):H1263–H1269.
11. Wang X, Fisher PW, Xi L, Kukreja RC (2008) Essential role of mitochondrial Ca2+-activated and ATP-sensitive K+ channels in sildenafil-induced late cardioprotection. *J Mol Cell Cardiol* 44(1):105–113.
12. Xu W, et al. (2002) Cytoprotective role of Ca2+- activated K+ channels in the cardiac inner mitochondrial membrane. *Science* 298(5595):1029–1033.
13. Sato T, Saito T, Saegusa N, Nakaya H (2005) Mitochondrial Ca2+-activated K+ channels in cardiac myocytes: A mechanism of the cardioprotective effect and modulation by protein kinase A. *Circulation* 111(2):198–203.
14. O'Rourke B (2007) Mitochondrial ion channels. *Annu Rev Physiol* 69:19–49.
15. Murry CE, Jennings RB, Reimer KA (1986) Preconditioning with ischemia: A delay of lethal cell injury in ischemic myocardium. *Circulation* 74(5):1124–1136.
16. Murphy E, Steenbergen C (2008) Mechanisms underlying acute protection from cardiac ischemia-reperfusion injury. *Physiol Rev* 88(2):581–609.
17. Quinlan CL, et al. (2008) Conditioning the heart induces formation of signalosomes that interact with mitochondria to open mitoKATP channels. *Am J Physiol Heart Circ Physiol* 295(3):H953–H961.
18. Insel PA, Patel HH (2009) Membrane rafts and caveolae in cardiovascular signaling. *Curr Opin Nephrol Hypertens* 18(1):50–56.
19. Fischmeister R, et al. (2006) Compartmentation of cyclic nucleotide signaling in the heart: The role of cyclic nucleotide phosphodiesterases. *Circ Res* 99(8):816–828.
20. Willoughby D, Cooper DM (2007) Organization and Ca2+ regulation of adenylyl cyclases in cAMP microdomains. *Physiol Rev* 87(3):965–1010.
21. Maurice DH, et al. (2014) Advances in targeting cyclic nucleotide phosphodiesterases. *Nat Rev Drug Discov* 13(4):290–314.
22. Juhaszova M, et al. (2009) Role of glycogen synthase kinase-3beta in cardioprotection. *Circ Res* 104(11):1240–1252.
23. Hayashi T, Rizzuto R, Hajnoczky G, Su TP (2009) MAM: More than just a housekeeper. *Trends Cell Biol* 19(2):81–88.

24. Ruiz-Meana M, Fernandez-Sanz C, Garcia-Dorado D (2010) The SR-mitochondria interaction: A new player in cardiac pathophysiology. *Cardiovasc Res* 88(1):30–39.
25. Odagiri K, et al. (2009) Local control of mitochondrial membrane potential, permeability transition pore and reactive oxygen species by calcium and calmodulin in rat ventricular myocytes. *J Mol Cell Cardiol* 46(6):989–997.
26. Ziman AP, Gómez-Viquez NL, Bloch RJ, Lederer WJ (2010) Excitation-contraction coupling changes during postnatal cardiac development. *J Mol Cell Cardiol* 48(2): 379–386.
27. Beca S, et al. (2013) Phosphodiesterase type 3A regulates basal myocardial contractility through interacting with sarcoplasmic reticulum calcium ATPase type 2a signaling complexes in mouse heart. *Circ Res* 112(2):289–297.
28. Tsutsumi YM, et al. (2008) Cardiac-specific overexpression of caveolin-3 induces endogenous cardiac protection by mimicking ischemic preconditioning. *Circulation* 118(19):1979–1988.
29. Fridolfsson HN, et al. (2012) Mitochondria-localized caveolin in adaptation to cellular stress and injury. *FASEB J* 26(11):4637–4649.
30. Hagiwara Y, et al. (2000) Caveolin-3 deficiency causes muscle degeneration in mice. *Hum Mol Genet* 9(20):3047–3054.
31. Horikawa YT, et al. (2008) Caveolin-3 expression and caveolae are required for isoflurane-induced cardiac protection from hypoxia and ischemia/reperfusion injury. *J Mol Cell Cardiol* 44(1):123–130.
32. Juhaszova M, et al. (2004) Glycogen synthase kinase-3beta mediates convergence of protection signaling to inhibit the mitochondrial permeability transition pore. *J Clin Invest* 113(11):1535–1549.
33. Yan C, Miller CL, Abe J (2007) Regulation of phosphodiesterase 3 and inducible cAMP early repressor in the heart. *Circ Res* 100(4):489–501.
34. Boengler K, et al. (2009) Presence of connexin 43 in subsarcolemmal, but not in interfibrillar cardiomyocyte mitochondria. *Basic Res Cardiol* 104(2):141–147.
35. Boengler K, et al. (2005) Connexin 43 in cardiomyocyte mitochondria and its increase by ischemic preconditioning. *Cardiovasc Res* 67(2):234–244.
36. Rodriguez-Sinovas A, et al. (2006) Translocation of connexin 43 to the inner mitochondrial membrane of cardiomyocytes through the heat shock protein 90-dependent TOM pathway and its importance for cardioprotection. *Circ Res* 99(1): 93–101.
37. Palmer JW, Tandler B, Hoppel CL (1986) Heterogeneous response of subsarcolemmal heart mitochondria to calcium. *Am J Physiol* 250(5 Pt 2):H741–H748.
38. Schroeder F, et al. (1991) Membrane cholesterol dynamics: Cholesterol domains and kinetic pools. *Proc Soc Exp Biol Med* 196(3):235–252.
39. Patel HH, Murray F, Insel PA (2008) Caveolae as organizers of pharmacologically relevant signal transduction molecules. *Annu Rev Pharmacol Toxicol* 48:359–391.
40. Han R, Campbell KP (2007) Dysferlin and muscle membrane repair. *Curr Opin Cell Biol* 19(4):409–416.
41. Cai C, et al. (2009) Membrane repair defects in muscular dystrophy are linked to altered interaction between MG53, caveolin-3, and dysferlin. *J Biol Chem* 284(23): 15894–15902.
42. Nguyen T, et al. (2012) Acute inhibition of GSK causes mitochondrial remodeling. *Am J Physiol Heart Circ Physiol* 302(11):H2439–H2445.
43. Sun B, et al. (2007) Role of phosphodiesterase type 3A and 3B in regulating platelet and cardiac function using subtype-selective knockout mice. *Cell Signal* 19(8): 1765–1771.
44. Begum N, Hockman S, Manganiello VC (2011) Phosphodiesterase 3A (PDE3A) deletion suppresses proliferation of cultured murine vascular smooth muscle cells (VSMCs) via inhibition of mitogen-activated protein kinase (MAPK) signaling and alterations in critical cell cycle regulatory proteins. *J Biol Chem* 286(29):26238–26249.
45. Zhang Z, et al. (2006) Reduced 6-month resource use and costs associated with cilostazol in patients after successful coronary stent implantation: Results from the Cilostazol for RESTenosis (CREST) trial. *Am Heart J* 152(4):770–776.
46. Katakami N, Kim YS, Kawamori R, Yamasaki Y (2010) The phosphodiesterase inhibitor cilostazol induces regression of carotid atherosclerosis in subjects with type 2 diabetes mellitus: Principal results of the Diabetic Atherosclerosis Prevention by Cilostazol (DAPC) study: A randomized trial. *Circulation* 121(23):2584–2591.
47. Guirguis E, et al. (2013) A role for phosphodiesterase 3B in acquisition of brown fat characteristics by white adipose tissue in male mice. *Endocrinology* 154(9):3152–3167.
48. Steinberg SF, Brunton LL (2001) Compartmentation of G protein-coupled signaling pathways in cardiac myocytes. *Annu Rev Pharmacol Toxicol* 41:751–773.
49. Michel JJ, Scott JD (2002) AKAP mediated signal transduction. *Annu Rev Pharmacol Toxicol* 42:235–257.
50. Kerfant BG, et al. (2007) PI3Kgamma is required for PDE4, not PDE3, activity in subcellular microdomains containing the sarcoplasmic reticular calcium ATPase in cardiomyocytes. *Circ Res* 101(4):400–408.
51. Ghigo A, et al. (2012) Phosphoinositide 3-kinase γ protects against catecholamine-induced ventricular arrhythmia through protein kinase A-mediated regulation of distinct phosphodiesterases. *Circulation* 126(17):2073–2083.
52. Tong H, Imahashi K, Steenbergen C, Murphy E (2002) Phosphorylation of glycogen synthase kinase-3beta during preconditioning through a phosphatidylinositol-3-kinase—dependent pathway is cardioprotective. *Circ Res* 90(4):377–379.
53. Das A, Xi L, Kukreja RC (2008) Protein kinase G-dependent cardioprotective mechanism of phosphodiesterase-5 inhibition involves phosphorylation of ERK and GSK3beta. *J Biol Chem* 283(43):29572–29585.
54. Young JC, Hoogenraad NJ, Hartl FU (2003) Molecular chaperones Hsp90 and Hsp70 deliver preproteins to the mitochondrial import receptor Tom70. *Cell* 112(1):41–50.
55. Ishikawa S, et al. (2012) Role of connexin-43 in protective PI3K-Akt-GSK-3β signaling in cardiomyocytes. *Am J Physiol Heart Circ Physiol* 302(12):H2536–H2544.
56. Cao CM, et al. (2010) MG53 constitutes a primary determinant of cardiac ischemic preconditioning. *Circulation* 121(23):2565–2574.
57. Wang X, et al. (2010) Cardioprotection of ischemia/reperfusion injury by cholesterol-dependent MG53-mediated membrane repair. *Circ Res* 107(1):76–83.
58. Song KS, et al. (1996) Expression of caveolin-3 in skeletal, cardiac, and smooth muscle cells. Caveolin-3 is a component of the sarcolemma and co-fractionates with dystrophin and dystrophin-associated glycoproteins. *J Biol Chem* 271(25):15160–15165.
59. Parton RG, Way M, Zorzi N, Stang E (1997) Caveolin-3 associates with developing T-tubules during muscle differentiation. *J Cell Biol* 136(1):137–154.
60. Ahmad F, et al. (2015) Regulation of SERCA2 activity by PDE3A in human myocardium: Phosphorylation-dependent interaction of PDE3A1 with SERCA2. *J Biol Chem* 290(11):6763–6776.
61. Ahmad F, et al. (2007) Insulin-induced formation of macromolecular complexes involved in activation of cyclic nucleotide phosphodiesterase 3B (PDE3B) and its interaction with PKB. *Biochem J* 404(2):257–268.
62. Ahmad F, et al. (2009) Differential regulation of adipocyte PDE3B in distinct membrane compartments by insulin and the beta3-adrenergic receptor agonist CL316243: Effects of caveolin-1 knockdown on formation/maintenance of macromolecular signalling complexes. *Biochem J* 424(3):399–410.
63. Perino A, Ghigo A, Scott JD, Hirsch E (2012) Anchoring proteins as regulators of signaling pathways. *Circ Res* 111(4):482–492.
64. Perino A, et al. (2011) Integrating cardiac PIP3 and cAMP signaling through a PKA anchoring function of p110γ. *Mol Cell* 42(1):84–95.
65. Patrucco E, et al. (2004) PI3Kgamma modulates the cardiac response to chronic pressure overload by distinct kinase-dependent and -independent effects. *Cell* 118(3): 375–387.
66. Perrino C, Rockman HA, Chiariello M (2006) Targeted inhibition of phosphoinositide 3-kinase activity as a novel strategy to normalize beta-adrenergic receptor function in heart failure. *Vascul Pharmacol* 45(2):77–85.
67. Mangiafico RA, Fiore CE (2009) Current management of intermittent claudication: The role of pharmacological and nonpharmacological symptom-directed therapies. *Curr Vasc Pharmacol* 7(3):394–413.
68. Packer M, et al.; The PROMISE Study Research Group (1991) Effect of oral milrinone on mortality in severe chronic heart failure. *N Engl J Med* 325(21):1468–1475.
69. Oikawa M, et al. (2013) Cyclic nucleotide phosphodiesterase 3A1 protects the heart against ischemia-reperfusion injury. *J Mol Cell Cardiol* 64:11–19.
70. Ye Y, et al. (2013) Phosphodiesterase-3 inhibition augments the myocardial infarct size-limiting effects of exenatide in mice with type 2 diabetes. *Am J Physiol Heart Circ Physiol* 304(1):H131–H141.
71. Birnbaum Y, et al. (2012) Phosphodiesterase III inhibition increases cAMP levels and augments the infarct size limiting effect of a DPP-4 inhibitor in mice with type-2 diabetes mellitus. *Cardiovasc Drugs Ther* 26(6):445–456.
72. Wechsler J, et al. (2002) Isoforms of cyclic nucleotide phosphodiesterase PDE3A in cardiac myocytes. *J Biol Chem* 277(41):38072–38078.
73. Hambleton R, et al. (2005) Isoforms of cyclic nucleotide phosphodiesterase PDE3 and their contribution to cAMP hydrolytic activity in subcellular fractions of human myocardium. *J Biol Chem* 280(47):39168–39174.